Supporting Information

Ahn *et al.* 10.1073/pnas.0803790105

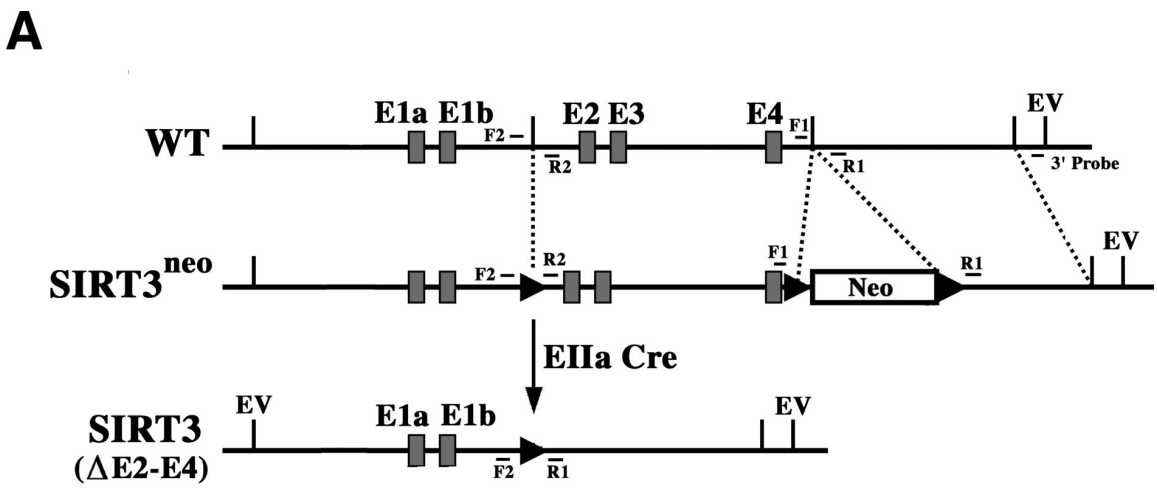

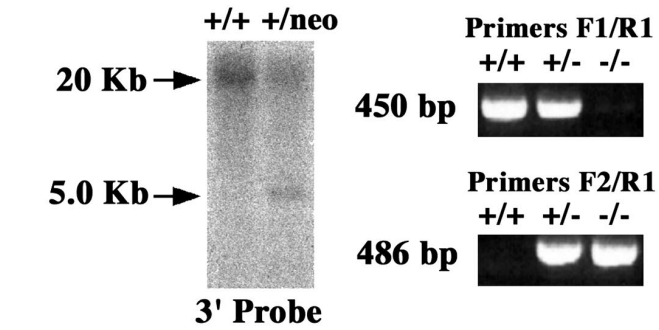

C

Crossing	$SIRT3^{+/-}$ × $SIRT3^{+/-}$		
Offspring	Total No. : 68		
Genotype	+/+	+/-	-/-
Predicted No.	17 (25%)	34 (50%)	17 (25%)
Actual No.	14	38	16

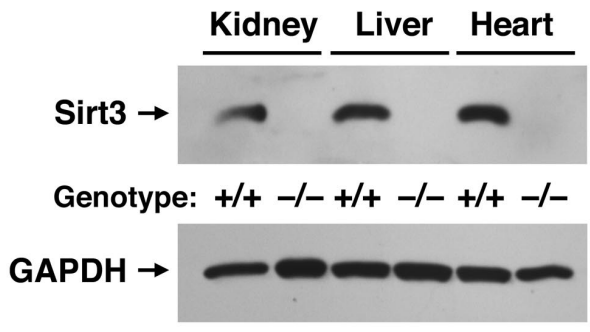

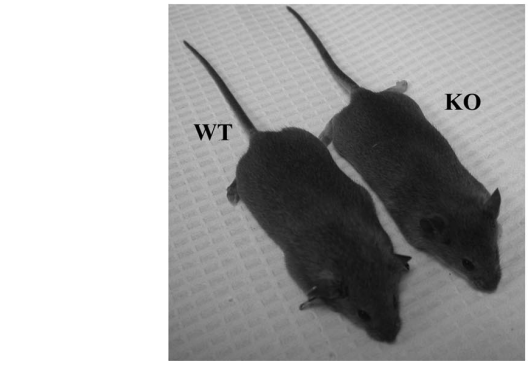

Fig. S1. Targeted disruption of the *Sirt3* gene. (*A*) Schematic of *Sirt3* gene-targeting strategy. Arrowhead, loxp sites; Neo, Neomycin gene; F1, R1, F2, and R2, positions of primers for genotyping; EV, EcoRV restriction site. Mice heterozygous for ploxPneo insertion ($Sirt3^{+/neo}$) were crossed with mice carrying a EIIa-Cre transgene to deleted exons 2–4 of Sirt3. (*B*) Southern blot analysis of genomic DNA from ES cells to identify correctly targeted ES clones and PCR genotyping of mice using primer pairs F1/R1 and F2/R1. F1/R1 detects a 450-bp band from wild-type and $Sirt3^{+/\Delta E2\text{-}E4}$ (+/−) mice, and F2/R1 detects a 486-bp band from +/−, and $Sirt3^{\Delta E2\text{-}E4/\Delta E2\text{-}E4}$ (−/−) mice. (*C*) Predicted and actual genotypes of offspring from $Sirt3^{+/-}$ intercrosses determined 4 weeks after birth. (*D*) Sirt3 protein expression from 50 μg of total protein from the indicated organs obtained from wild-type or $Sirt3^{-/-}$ mice. (*E*) Example of 8-week-old littermate pairs of wild-type and $Sirt3^{-/-}$ mice that appear indistinguishable.

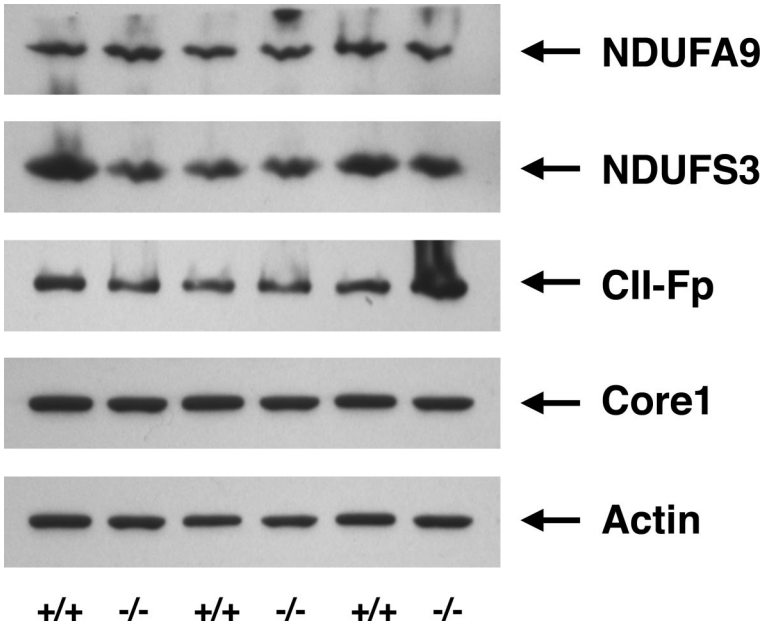

Fig. S2. Assessment of expression levels of various components of the ETC in wild-type and Sirt3$^{-/-}$ mice. Liver protein lysate (40 μg) was used for Western blot analysis to determine the expression levels of various components of the ETC. Analysis was performed for three wild-type (+/+) or Sirt3$^{-/-}$ mice. Analysis of Complex I components (NDUFA9 and NDUFS3), Complex II (CII-Fp), and the 49-kDa Core 1 protein of Complex III is shown. Although there are slight variations between mice, in general, expression of these various components of the ETC appear to be similar in wild-type and Sirt3$^{-/-}$ mice.

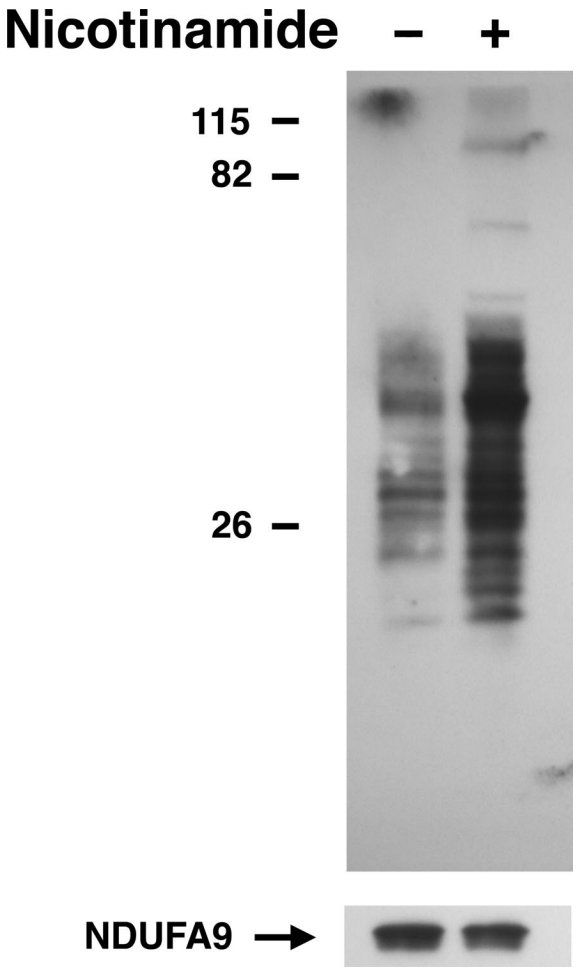

Fig. S3. Nicotinamide treatment increases Complex I acetylation. Immunocapture of Complex I from equal amount of HeLa cell lysate either untreated (−) or treated with nicotinamide (10 mM for 16 h). Immunocaptured Complex I was then run on an SDS/PAGE, transferred to a solid membrane, and probed for acetyl-lysine residues. Equivalent levels of immunocaptured Complex I was confirmed by probing for the level of the Complex I component NDUFA9 for both conditions.

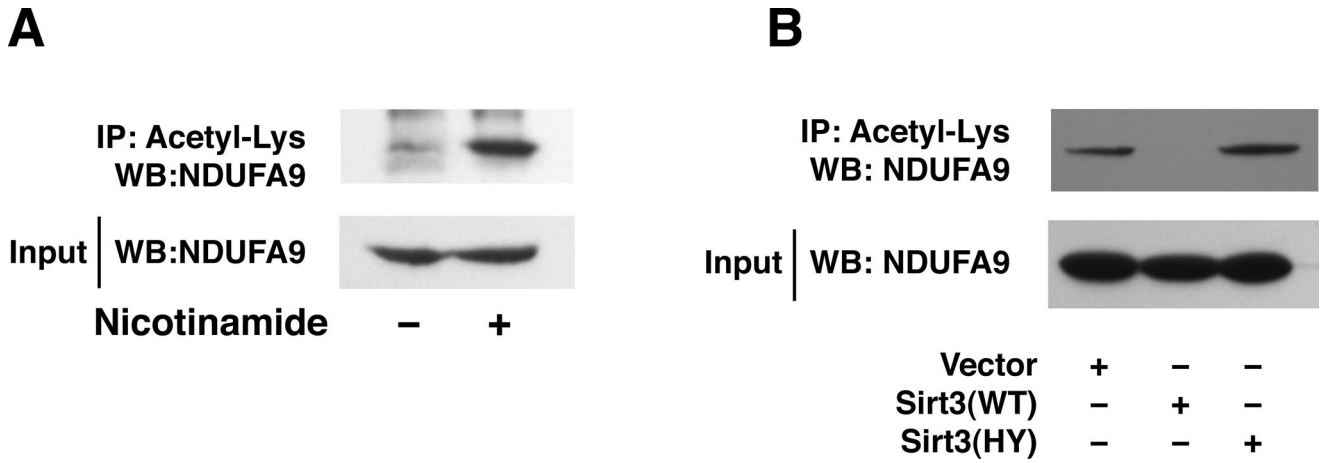

Fig. S4. Regulation of NDUFA9 acetylation. (*A*) Acetylation of NDUFA9 in HeLa cell treated or untreated with nicotinamide (10 mM for 16 h). Equal amounts of total protein lysate were immunoprecipitated with an acetyl-lysine antibody, and the immunoprecipitated proteins were subsequently assessed for the amount of NDUFA9. (*B*) Levels of NDUFA9 acetylation in HeLa cells transfected 48 h earlier with an empty vector, wild-type Sirt3, or the deactetylase inactive mutant (HY) of Sirt3.

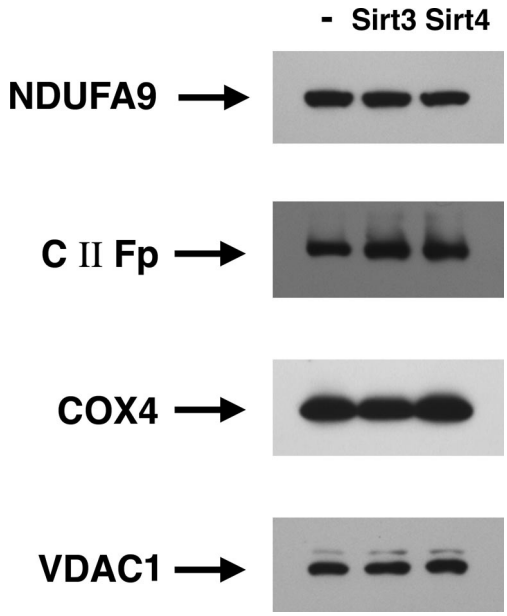

Fig. S5. Levels of mitochondrial protein after *in vitro* treatment with purified sirtuins. Mitochondria from HeLa cells were incubated with purified Flag-Sirt3, Flag-Sirt4, or Flag-vector (−), and the modified mitochondria were then assessed for Complex I activity (see Fig. 3*E*). To confirm that equal amounts of mitochondria were being analyzed in these Complex I activity assays, a portion (75 μg) of the *in vitro*-modified mitochondria reaction mixtures were analyzed by Western blot. Shown here are analysis of expression of NDUFA9 (Complex I), CII-Fp (Complex II), COX IV (a component of Cytochrome *c* oxidase), and VDAC1 (a non-ETC mitochondrial protein) from each of the three reaction mixtures.

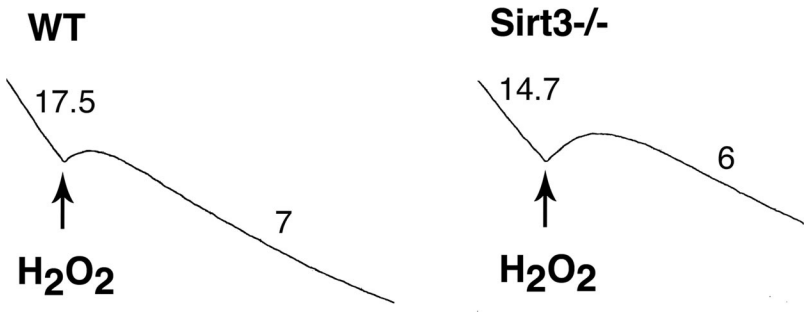

Fig. S6. Measurement of whole-cell respiration in wild-type (WT) and Sirt3$^{-/-}$ MEFs. Arrow indicates the addition of hydrogen peroxide (0.5 mM). Basal respiration was consistently reduced in Sirt3$^{-/-}$ MEFs (percent reduction was 27 $\pm$ 2%, $n = 4$; $P < 0.01$). However, after oxidative stress, respiration was similarly reduced in both cell types. Respiration rates are shown numerically and are expressed in units of nmol of O_2 per minute per 10^6 cells. Results are from one of two similar experiments.

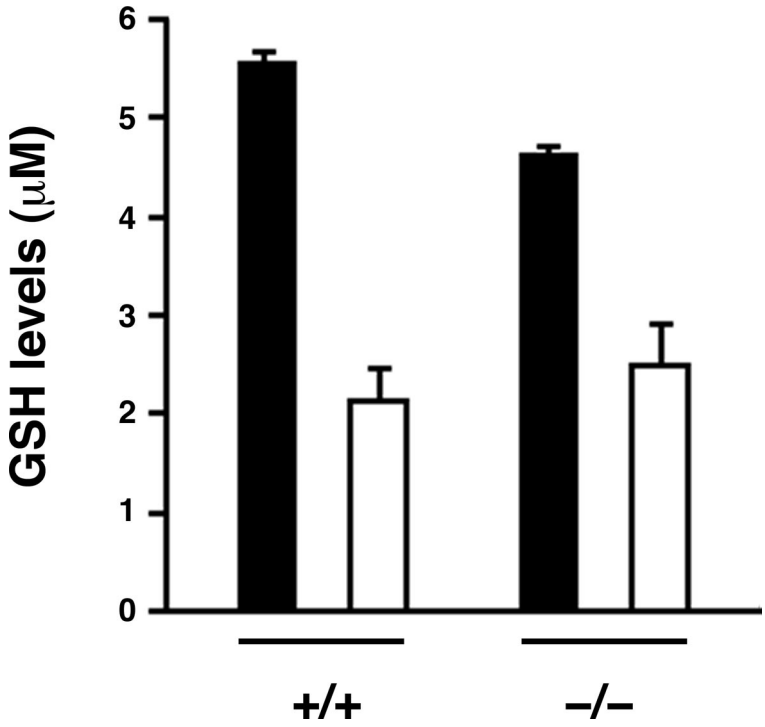

Fig. S7. Levels of glutathione in wild-type or Sirt3$^{-/-}$ MEFs under basal conditions (shaded bars) or following hydrogen peroxide treatment (0.5 mM for 30 min; white bars). Results are the mean ± SD of three separate experiments.

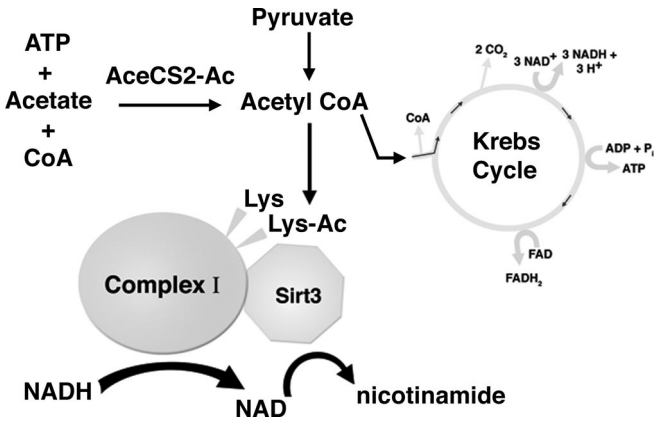

Fig. S8. A model for Sirt3 regulation of mitochondrial homeostasis. Sirt3 is capable of direct interaction with Complex I, a multisubunit complex that functions as an NADH dehydrogenase. NAD generated by Complex I might, in turn, be important in regulating Sirt3 activity. In addition, previous reports have identified the enzyme AceCS2 as a target for Sirt3 deacetylation. This enzyme is capable of generating Acetyl CoA that is used both for intermediary metabolism via the Krebs cycle and in protein acetylation (Ac). The coordinated effects of Sirt3 through deacetylation of enzymes involved in both substrate generation (AceCS2, GDH, and others) and substrate utilization (e.g., Complex I) are required to maintain resting ATP levels.

Table S1. Measured respiration in state III and state IV for WT and Sirt3$^{-/-}$ (KO) hepatic mitochondria by using a Complex I substrate (glutamate + malate) or a Complex II substrate (succinate) in the presence of rotenone to prevent reverse electron flow

	Glutamate + malate			Succinate + rotenone		
Genotype	State III	State IV	RCR	State III	State IV	RCR
KO	141.5 ± 11.3*	24.5 ± 2.3	5.8	229.5 ± 16.8	71.3 ± 13.3	3.2
WT	174 ± 9.1	26.1 ± 2.5	6.7	223 ± 16.4	65.3 ± 12.9	3.4

Measurements are measured in nmol of O_2 per minute per milligram of protein and are the mean ± SD of four littermates. RCR, respiratory control ratio.